SPALL FRACTURE IN DUCTILE METALS

Z. Bílek*, R. Cortéz+, J. Buchar* and M. Elices+

The optical and scanning electron microscopy have been used to characterise the structural features following high strain rate ($> 10^6 s^{-1}$) deformation resulting from explosive loading. Particular attention is paid to the metallurgical aspects of spalling in copper, aluminium and low carbon steel. Quantitative spall fracture criterions predicting the extent of damage have been successfully compared with experimental observations, by incorporating them into finite difference computer code.

INTRODUCTION

Spall damage is a type of fracture produced when large tensile stresses are developed in material bodies as a result of the interaction of stress waves. The damage develops independently at various points in the body since the short duration of stress application, but interacts in a complicated way with the stress wave. Dynamic loads which may produce spall damage result from high velocity impact, detonation of high intensity explosives and short term radiation deposition. Damage levels ranging from a few small cracks or voids to complete comminition of regions of the body are produced under varying conditions. Various aspects of the spall problem have been reviewed (1-3) and many attempts have been made to develop a predictive capability for spall damage.

* Institute of Metallurgy, CAS, 616 62 Brno, Zizkova 22 Czechoslovakia

+ Departmento De Fisica De Materiáles, Ciudad Universitaria - 28040 Madrid, Spain

This paper describes the results of a study of the spall damage and fracture development in aluminium, copper and steel applying experimental and computational procedures. Experiments are modelled numerically by finite difference computer code incorporating the various spall fracture criterions and predicted final damage distributions are compared with experimental findings. The good agreement of both supports the validity of the theoretical approach taken.

EXPERIMENTAL PROCEDURE

From the given materials the cylindrical specimens with diameter of 100 mm and height of 30 mm were prepared. These specimens were loaded with help of the explosive charge as shown in Fig. 1. The basic parameters of explosives used are reported in Table 1.

Table 1 - Properties of explosive used in our experiments

Explosives	Heat of explosion [kJ/g]	Detonation velocity [m/s]	Density [g/cm^3]
Semtex S35	2050	2750	1.1
Semtex 2	1420	5500	2.2
Semtex 1A	4970	7400	1

The loading pressure time were recorded by the manganin foil gauges up to the maximum values p_m. The materials studied were copper, aluminium and steel (close to armco iron). Cu included some impurities 0.006 % Fe and 0.38 % Zn. Initial density was $\varrho = 8.93$ g cm^{-3}, Poisson ratio $\nu = 0.33$, Young's modulus $E = 1.19 \times 10^5$ MPa, yield stress (Hugoniot elastic limit) $\sigma_y = 0.9$ GPa, thermal expansion coefficient $\alpha = 49.5 \times 10^{-6}$ $^oC^{-1}$, thermal conductivity $k = 394$ Wm^{-1} $^oK^{-1}$, specific heat $c_p = 0.092$ cal g^{-1} $^oC^{-1}$ and Grüneisen parameter $\gamma = 1.99$. Al was contaminated by 0.02 % Mn, 0.002 % Mg, 0.14 % Fe, 0.002 % Zn. The basic properties were: $\varrho = 2.7$ g cm^{-3}, $\nu = 0.35$, $E = 7.05 \times 10^4$ MPa, $\sigma_y = 300$ MPa, $\alpha = 6.9 \times 10^{-5}$ $^oC^{-1}$, $k = 249$ Wm^{-1} $^oK^{-1}$, $c_p = 0.23$ cal g^{-1} ^oC and $\gamma = 2.25$.

Steel had the following chemical composition: 0.082 % ^oC, 0.23 % Mn, 0.019 % P, 0.026 % S, 0.03 % Cr and 0.05 % Ni. The basic characteristics are: ϱ =

$= 7.85$ g cm^{-3}, $\nu = 0.28$, $E = 2.1 \times 10^5$ MPa, $\sigma_y = 1.067$ GPa, $\alpha = 35.1 \times 10^{-6}$ $^oC^{-1}$, $k = 54$ Wm^{-1} $^oK^{-1}$, $c_p = 0.107$ cal g^{-1} $^oC^{-1}$, $\gamma = 1.69$.

The fracture damage produced by the stress pulses was quantitatively assesed in the following way: recovered specimens were sectioned on a diameter and the section surface was grounded and polished to reveal the fracture pattern. The main attention was focused on the identification of crack initiation sites. The fracture damage was analyzed quantitatively by counting nad measuring the traces of the microfractures on the polished surface.

COMPUTATIONAL PROCEDURE

For numerical simulations of spall fracture the thermo-mechanical calculations were made by using PR2D finite difference code (4) with explicit time integration. The mesh used for computations is shown in Fig.2 and consists of 924 quadrilateral cells covering one half of the symmetrical specimen. A mixed discretization procedure was employed. The behaviour of Cu was described by the state equation

$$p = a_1 \left(\frac{V_0}{V} - 1 \right)^n \qquad (1)$$

relating the pressure to the initial volume V_0 and volume V, $a_1 = 278.2$ GPa and $n = 1.2$. The following spall fracture criterion was used

$$\int_0^t (\sigma - \sigma_b)^n \, dt \geq K_c \qquad (2)$$

where the values of materials constants were taken as $n = 2$, $K_c = 1.9 \times 10^{-7}$ GPa s and the treshold stress $\sigma_b = -0.75$ GPa.

The behaviour of Al was described by the state equation

$$p = a_1 \left(\frac{V_0}{V} - 1 \right) + a_2 \left(\frac{V_0}{V} - 1 \right)^2 \qquad (3)$$

where $a_1 = 7.75 \times 10^4$ MPa and $a_2 = 15.5 \times 10^4$ MPa. Critical fracture stress criterion was adopted

$$\sigma \geq \sigma_{SPALL} \qquad (4)$$

to characterise the damage development. The critical stresses σ_{SPALL} are given in Table 2.

Table 2 - The values of σ_{SPALL} at different temperatures T .

T [°C]	0	15	200	400	500
σ_{SPALL}	3	2.7	2.4	1.9	0.8

Our steel behaves according eq. (1) where a_1 = = 305.18 GPa and n = 1.33. Fracture was controlled by criterion (4) with σ_{SPALL} = 1.4 GPa at 15 °C and σ_{SPALL} = 1.2 GPa at T = 80 °C. The loading pressure pulses were introduced into the computer code in the form of table directly obtained from the experimental measurements.

RESULTS AND DISCUSSION

Since the limited scope of this paper only selected results are presented here and for more details we refer the interested readers to another our article (5). Fig. 3 indicate the development of spalling in Al as dependent upon loading conditions. Incipient spall in Al is shown in Fig. 4. Numerical model corresponding to the loading conditions for the third specimen from the top in Fig. 3 (i.e. p_m = 8.4 GPa) is shown in Fig. 5 and good agreement of spall fracture extent is observed. Also, numerical prediction of multiple spall in steel agrees quite well with the experimental evidence, both shown in Fig. 6. Fig. 7 demonstrates the complicated way of materials loading at different points. Also, strain rate is far from uniform - Fig. 8. Intensive plastic straining produces the temperature rise calculated in Fig. 9.

Even the general features of spall fracture development can be predicted numericaly, the further refiment is needed to model property incipient spall nucleation on the microscopic level.

REFERENCES

(1) Meyers, M.A. and Aimone, C.T., Progr. Mat. Scie. Vol. 28, 1983, pp. 2-91.

(2) Curran, D.R., Seaman, L. and Shockey, D.A., Physics Reports Vol. 147, 1987, pp. 253-388.

(3) Buchar, J., Bílek, Z. and Dušek, F., Mechanical

Behaviour of Metals at Extremely High Strain Rates Trans. Tech. Publ. 1986, Switzerland.

(4) Principia, S.A., PR2D User's guide, 1987, Madrid Spain.

(5) Cortéz, R. et al., Int. J. Impact Eng., in preparation.

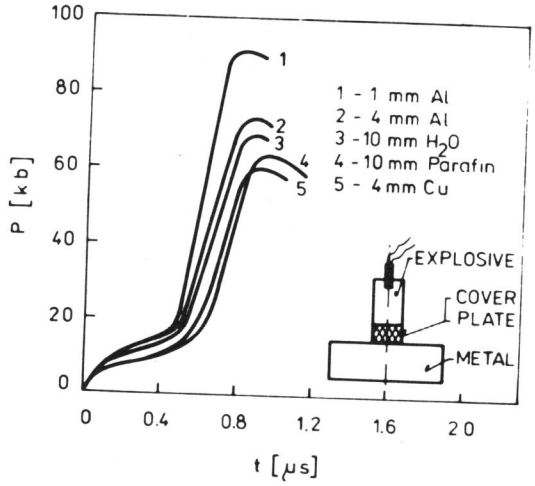

Figure 1 Experimental arrangement for the investigation of explosive loading. The effect of an inter layer upon the development of the pressure distribution

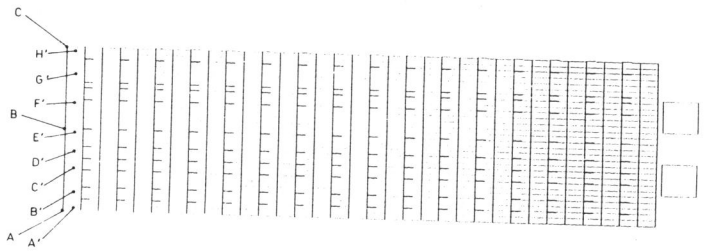

Figure 2 Finite difference mesh used in the numerical analysis

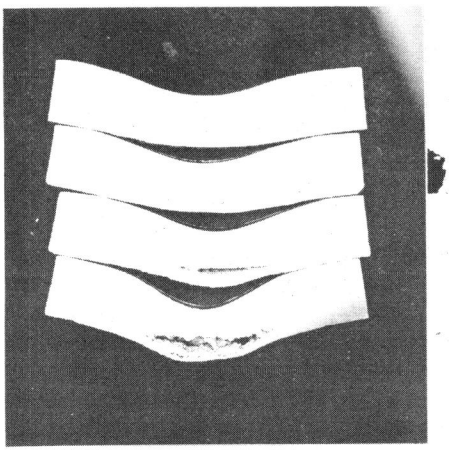

Figure 3 Dependence of spall fracture nucleation and growth upon loading conditions

Figure 4 Incipient spall in Al

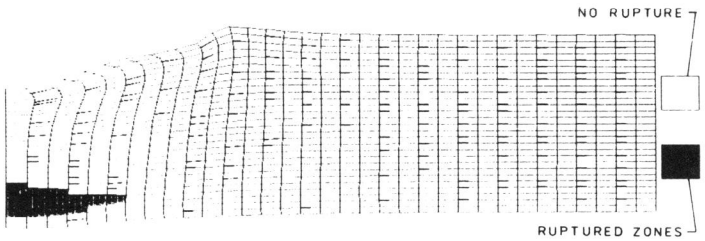

Figure 5 Numerical model of spall fracture development in Al

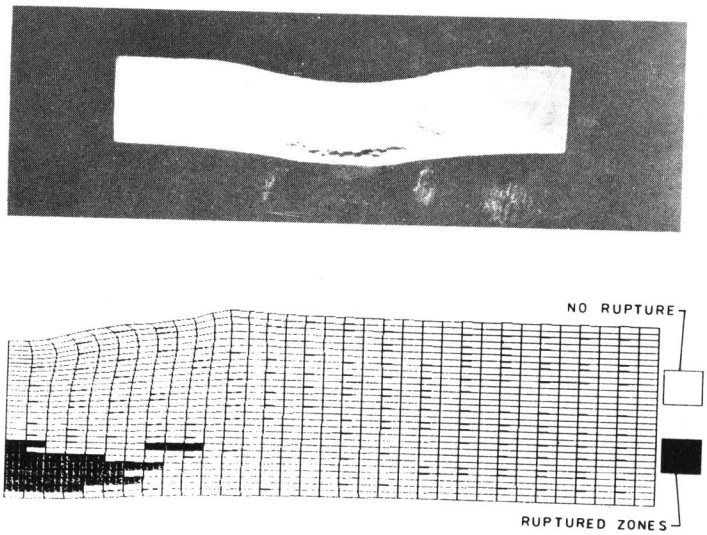

Figure 6 Multiple spall in steel and its numerical simulation for p_m = 14.9 GPa

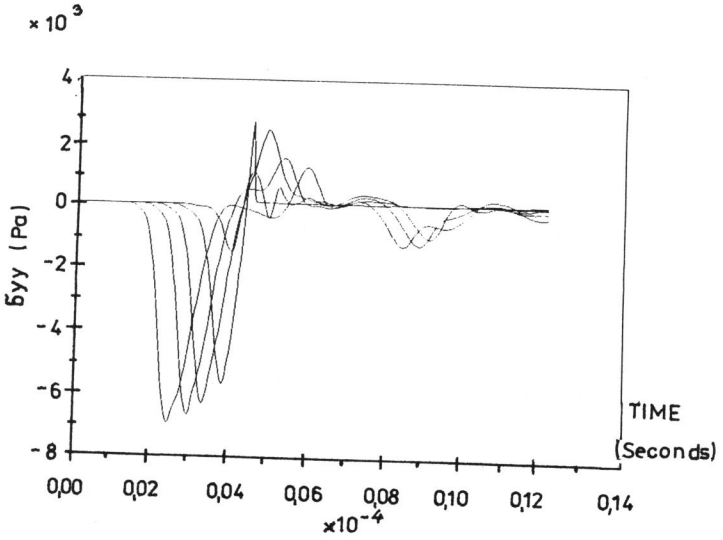

Figure 7 Dependence of axial stress component σ_{yy} on time at points E, D, C, B from right to left, (Al)

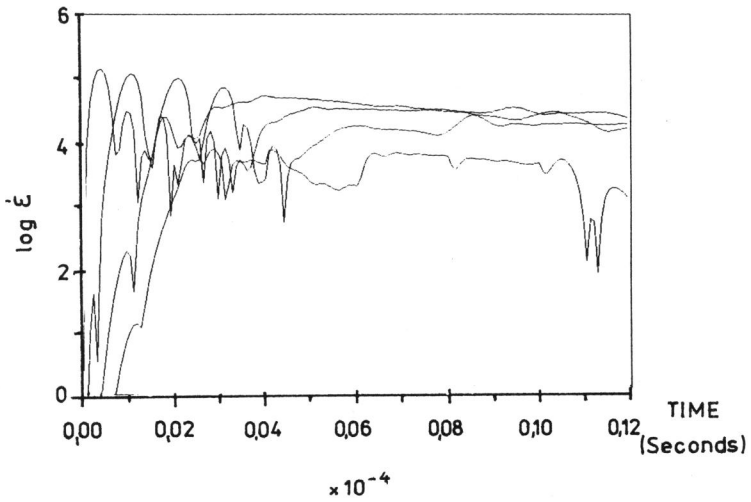

Figure 8 Strain rate distribution at cells E, F, G, H (from right to left) for copper, p_m = 10 GPa

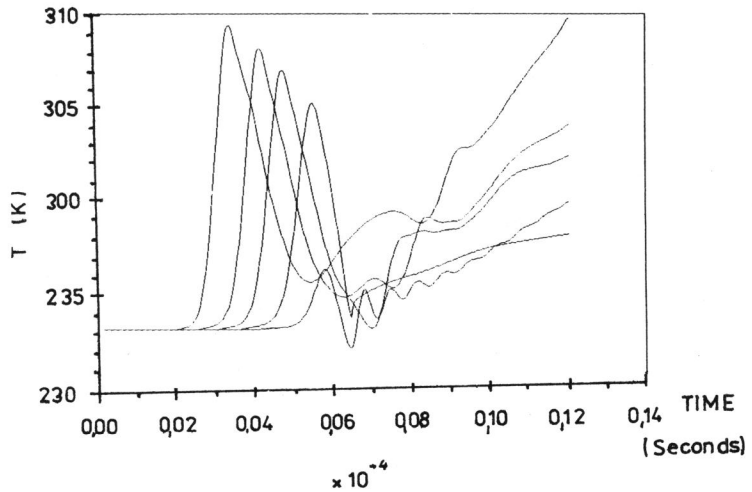

Figure 9 Temperature rise during explosive loading of copper specimen at cells A, B, C, D, E from right to left